Efficient Bound Tightening Techniques for Convex Relaxations of AC Optimal Power Flow

Dmitry Shchetinin, *Student Member,* Tomas Tinoco De Rubira, *Member,* Gabriela Hug, *Senior Member*

***Abstract*—Convex relaxations of the AC optimal power flow problem in certain cases can recover a globally optimal point of the original problem. However, in general their solutions are not guaranteed to be physically meaningful. While the relaxation quality can be improved by enforcing tighter bounds on variables, existing bound tightening methods do not scale well with grid size. This paper presents three methods for tightening bounds on branch angle differences that complement each other and are highly parallelizable. The proposed methods are computationally efficient even for large-scale grids and thus can be used as a preprocessing step before solving the convex relaxation of the optimal power flow problem. Numerical experiments demonstrate that these methods can significantly tighten most of the bounds in a fraction of the time required to solve the convex relaxation. In addition, the experimental results show that tighter bounds improve the relaxation quality and reduce the optimality gap.**

***Index Terms*—bound tightening, convex relaxation, optimal power flow**

I. Introduction

THE AC Optimal Power Flow (OPF) problem is a non-linear, non-convex optimization problem, which was first formulated by Carpentier in [1] and has attracted significant attention since then. A comprehensive overview of proposed solution approaches can be found in [2], [3]. Despite considerable research efforts, solving the AC OPF problem efficiently and reliably for realistic grids remains a challenge due to its complexity and high dimensionality.

The past years have witnessed substantial improvements in general-purpose Nonlinear Programming (NLP) solvers. However, they still cannot always find a local optimum of the AC OPF problem [4], [5], which limits the widespread adoption of AC OPF by industry because system operators require reliable solution algorithms [6]. To enable the application of such algorithms, the power flow equations are typically linearized using the so-called DC approximation [7]–[9], thus leading to a convex optimization problem. However, the quality of the DC OPF solution is inherently limited due to inaccuracies introduced by linearization, which can be significant [10], [11]. Therefore, other approximation approaches are needed to make the approximate solution more useful.

Recently, the application of convex relaxations to the AC OPF problem has attracted significant attention of the research community. The idea is to relax the problem's feasible space in order to make it convex, thus enabling the application of reliable solution algorithms. In addition, the solution of the relaxation represents a lower bound on the actual solution. The proposed types of relaxations include semi-definite programming (SDP) [12], second-order cone (SOC) [13] and quadratic convex (QC) relaxations [14]. Tight relaxations, which exist for certain test systems and grid topologies, enable the recovery of a globally optimal solution of the original problem [15], [16]. However, in general the relaxations are not guaranteed to produce physically meaningful solutions for arbitrary power systems.

One way to improve the relaxation quality is to enforce tighter bounds on variables, which strengthens the relaxation. In [17], the authors use local information such as individual bus injections or line flow limits to tighten the bounds. While the proposed procedure is computationally efficient, its effect is limited because only some system elements are considered for tightening the bounds on a particular variable. In [18]–[20], the authors choose a different strategy and use the information of the entire system to tighten the individual variable bounds. This helps produce tighter bounds but in order to tighten each bound, one has to solve a convex optimization problem with a size of the same order as the original AC OPF problem. While individual bounds can be tightened in parallel, such an algorithm is computationally prohibitive for large-scale grids.

This paper addresses this problem by proposing three computationally efficient methods for tightening bounds on branch phase angle differences. The first method tightens the bounds on each angle difference using only the parameters of the corresponding branch, resulting in linear complexity with respect to the system size. The other two methods tighten a particular bound by formulating a convex optimization problem that includes the information of the entire system and admits a fast analytical solution. All three proposed methods complement each other and are highly parallelizable. They are made publicly available as an open-source MATLAB-based package. Due to their low computational complexity, these methods are applicable to large-scale grids and can be used as a preprocessor prior to solving the convex relaxation of the AC OPF problem. The paper analyses the efficiency and efficacy of these methods as well as their impact on the quality of the QC relaxation using a number of large-scale test grids.

The rest of the paper is structured as follows. Sections II and III present the formulations of the AC OPF problem and its QC relaxation, respectively. Section IV describes the proposed bound tightening methods. Section V briefly discusses the implementation of the developed algorithms. Section VI presents the results of numerical experiments and Section VII provides the summary.

II. Formulation of AC OPF Problem

The goal of the AC OPF problem is to find an operating point that satisfies physical and operational constraints and is optimal with respect to a given objective. This work considers the minimization of the total supply cost in the system. The supply cost of the i-th generator is modeled as a quadratic function of its active power output P_{G_i}:

$$C_i(P_{G_i}) := c_{2_i} P_{G_i}^2 + c_{1_i} P_{G_i} + c_{0_i}, \tag{1}$$

where $c_{2_i} \geq 0, c_{1_i}, c_{0_i}$ are machine-specific cost coefficients.

This paper considers active P_G and reactive Q_G power outputs of generators as the only decision variables. The dependent variables are bus voltage magnitudes V and phase angles θ. In practice, various control devices are present in the system and could be included as variables in the OPF problem [6]. To limit the scope of the paper, these devices as well as contingencies are not included in the formulation.

In order to ensure that the AC OPF solution satisfies Kirchhoff's laws, nodal power balance equations are included in the problem in the form of equality constraints. The optimization problem also contains several types of inequality constraints. Bus voltage magnitudes, generator outputs and branch phase angle differences have upper and lower bounds dictated by the physical properties of the equipment and stability issues. Line flows have so-called thermal limits based on the maximum allowed temperature of the wires. This study models these limits by imposing bounds on the magnitudes I of line currents, which is what is typically done by system operators.

The considered AC OPF problem is formulated as follows:

$$\underset{P_G,Q_G,V,\theta}{\text{minimize}} \quad \sum_{i\in\mathcal{G}} C_i(P_{G_i}) \qquad \text{subject to} \tag{2a}$$

$$\sum_{k\in\mathcal{G}_i} P_{G_k} - P_{D_i} = \sum_{j\in\Omega_i} (G_{ij}V_iV_j\cos\theta_{ij} + B_{ij}V_iV_j\sin\theta_{ij}) + G_{ii}V_i^2, \quad i\in\mathcal{N} \tag{2b}$$

$$\sum_{k\in\mathcal{G}_i} Q_{G_k} - Q_{D_i} = \sum_{j\in\Omega_i} (G_{ij}V_iV_j\sin\theta_{ij} - B_{ij}V_iV_j\cos\theta_{ij}) - B_{ii}V_i^2, \quad i\in\mathcal{N} \tag{2c}$$

$$P_{G_i}^{\min} \le P_{G_i} \le P_{G_i}^{\max}, \quad i\in\mathcal{G} \tag{2d}$$

$$Q_{G_i}^{\min} \le Q_{G_i} \le Q_{G_i}^{\max}, \quad i\in\mathcal{G} \tag{2e}$$

$$V_i^{\min} \le V_i \le V_i^{\max}, \quad i\in\mathcal{N} \tag{2f}$$

$$\theta_{ij}^{\min} \le \theta_{ij} \le \theta_{ij}^{\max}, \quad (i,j)\in\mathcal{L} \tag{2g}$$

$$I_{ij}(V_i,V_j,\theta_{ij}) \le I_{ij}^{\max}, \quad (i,j)\in\mathcal{L} \tag{2h}$$

$$I_{ij}(V_i,V_j,\theta_{ij}) \le I_{ji}^{\max}, \quad (i,j)\in\mathcal{L} \tag{2i}$$

where $\mathcal{G}$, $\mathcal{N}$, and $\mathcal{L}$ are the sets of all generators, buses, and branches, respectively, Ω_i and $\mathcal{G}_i$ are the sets of all buses and generators connected to bus i, G and B are real and imaginary parts of the admittance matrix, respectively, $\theta_{ij} = \theta_i - \theta_j$ is the phase angle difference, P_{D_i} and Q_{D_i} are the active and reactive power demands at bus i, I_{ij} and I_{ji} are the magnitudes of the current at both ends of line (i,j).

Problem (2) is non-convex because of the power balance equations (2b)-(2c) and inequality constraints on branch current magnitudes (2h)-(2i). Therefore, local solvers are not guaranteed to find a globally optimal solution. To find the global optimum of problem (2), one can convexify it by replacing non-convex constraints with their convex relaxations. A number of relaxation approaches have been proposed in recent years, yet none can guarantee the tightness of relaxation for an arbitrary system. This paper focuses on the so-called quadratic convex (QC) relaxation and proposes methods to make it tighter, which improves the solution quality.

III. QC Relaxation of AC OPF Problem

The idea behind the QC relaxation is to replace the non-convex terms in problem (2) by their convex envelopes using the known bounds on variables. This will make the optimization problem convex at a cost of expanding its feasible space. Observe that constraints (2b)-(2c) are non-convex because of the nonlinear terms V_i^2, $V_iV_j\sin\theta_{ij}$, and $V_iV_j\cos\theta_{ij}$. The bounds on variables that enter these terms, namely voltage magnitudes and phase angle differences, are imposed by system operators. If the bounds on a particular θ_{ij} are not known, they can be safely assumed to be $\pm\pi/2$, which is a steady-state limit. In the following, superscripts l and u refer to the lower and upper bounds on a variable.

Let us consider each of the nonlinear terms mentioned above. The convex envelope of the square of a variable is given by

$$\left\langle x^2 \right\rangle := \begin{cases} \check{x} \ge x^2, \\ \check{x} \le \left(x^l + x^u\right) x - x^l x^u. \end{cases} \tag{3}$$

Thus, x^2 can be replaced by $\check{x}$ and two convex constraints defined in (3). The convex envelopes of $V_iV_j\sin\theta_{ij}$ and $V_iV_j\cos\theta_{ij}$ can be obtained by combining and nesting the convex envelopes of bilinear terms and the convex envelopes of trigonometric functions. The convex envelope of the bilinear term was proposed by McCormick in [21] and is defined as

$$\langle xy \rangle := \begin{cases} \check{xy} \ge x^l y + y^l x - x^l y^l, \\ \check{xy} \ge x^u y + y^u x - x^u y^u, \\ \check{xy} \le x^l y + y^u x - x^l y^u, \\ \check{xy} \le x^u y + y^l x - x^u y^l. \end{cases} \tag{4}$$

The convex envelopes of sine and cosine functions are presented in [14] and given by

$$\langle \sin(x) \rangle := \begin{cases} \check{sx} \le \cos(x^m)(x - x^m) + \sin(x^m), \\ \check{sx} \ge \cos(x^m)(x + x^m) - \sin(x^m). \end{cases} \tag{5}$$

$$\langle \cos(x) \rangle := \begin{cases} \check{cx} \le 1 - \frac{1-\cos(2x^m)}{(2x^m)^2} x^2, \\ \check{cx} \ge \gamma_c \left(x - x^l\right) + \cos(x^l), \end{cases} \tag{6}$$

where $x^m = \frac{\max\left\{|x^l|,|x^u|\right\}}{2}$ and $\gamma_c = \frac{\cos(x^l)-\cos(x^u)}{x^l - x^u}$. In [19], the reader can find more details on these envelopes and a tighter version of (5) for particular values of variable bounds.

The QC relaxation of the AC OPF problem is formulated as:

$$\text{minimize} \quad \sum_{i\in\mathcal{G}} C_i(P_{G_i}) \qquad \text{subject to} \tag{7a}$$

(2d) − (2i)

$$W_{ii} = \left\langle V_i^2 \right\rangle, \quad i\in\mathcal{N} \tag{7b}$$

$$W_{ij}^S = \left\langle \langle V_iV_j \rangle \langle \sin(\theta_{ij}) \rangle \right\rangle, \quad (i,j)\in\mathcal{L} \tag{7c}$$

$$W_{ij}^C = \left\langle \langle V_iV_j \rangle \langle \cos(\theta_{ij}) \rangle \right\rangle, \quad (i,j)\in\mathcal{L} \tag{7d}$$

$$\sum_{k\in\mathcal{G}_i} P_{G_k} - P_{D_i} = \sum_{j\in\Omega_i} (G_{ij}W_{ij}^C + B_{ij}W_{ij}^S) + G_{ii}W_{ii}, \quad i\in\mathcal{N} \tag{7e}$$

$$\sum_{k\in\mathcal{G}_i} Q_{G_k} - Q_{D_i} = \sum_{j\in\Omega_i} (G_{ij}W_{ij}^S - B_{ij}W_{ij}^C) - B_{ii}W_{ii}, \quad i\in\mathcal{N} \tag{7f}$$

$$\left(W_{ij}^S\right)^2 + \left(W_{ij}^C\right)^2 \le W_{ii}W_{jj}, \quad (i,j)\in\mathcal{L} \tag{7g}$$

Here, W_{ii}, W_{ij}^S, and W_{ij}^C represent the convex relaxations of V_i^2, $V_iV_j\sin\theta_{ij}$, and $V_iV_j\cos\theta_{ij}$ based on (3)-(6). Thus, the optimization variables include P_G, Q_G, V, θ, W, W^S, and W^C. Constraint (7g), which is a rotated second-order cone, is added to strengthen the relaxation [14]. Using other constraints to strengthen the relaxation is outside of the scope of the paper.

While problem (7) is convex, its feasible set is larger than the feasible set of problem (2). Therefore, the solution of (7) represents a lower bound on the value of the objective

function of the original problem. In addition, this solution is in general physically meaningless, i.e. it does not satisfy the power balance equations and cannot be implemented in the real system. To make it more useful, one has to improve the relaxation quality by making it as tight as possible. One way of doing it is to make the convex envelopes in (7b)-(7d) tighter, which can be done by enforcing tighter bounds on variables.

IV. Proposed Bound Tightening Techniques

The bounds on variables can be tightened using the knowledge of the feasible set of the original problem or its relaxation. For instance, to tighten the lower(upper) bound on a particular variable, one can solve the optimization problem with the objective of minimizing(maximizing) this variable subject to all or some constraints in the QC relaxation (7). This is the approach employed by the authors in [18], [19]. The bounds on all variables can be tightened in parallel and then this procedure can be repeated iteratively until no further tightening is possible. Clearly, the size of the optimization problem that needs to be solved to tighten each bound is proportional to the size of the power system (number of buses and branches) under consideration. Hence, this approach has a high computational cost and would require potentially thousands of parallel processors for large-scale systems.

This paper presents three bound tightening methods that are computationally efficient even for large-scale grids and thus can be used as a preprocessor before solving the convex relaxation of the AC OPF problem. These methods are designed to tighten the bounds on angle differences because they can be tightened more extensively than voltage magnitudes as was experimentally shown in [18]. Nevertheless, the paper will point out whether a particular proposed method can be used to tighten voltage magnitudes or their differences.

The first method is based on the properties of the feasible set of individual line flow constraints (2h)-(2i). The bounds on each θ_{ij} are tightened using only the corresponding line flow constraints at the beginning and end of the branch. Tightening each bound is constant-time and the overall computation time grows linearly with the number of branches in the system. In the other two methods, the information of the entire system is used to tighten a particular variable bound. The computational efficiency for these two methods is achieved by formulating an optimization problem for tightening a particular bound in a way that admits a fast solution.

Several points should be noted before moving to the detailed description of the proposed bound tightening methods. First, the paper primarily focuses on the computational efficiency, i.e. the presented techniques do not necessarily produce the tightest possible bounds. Second, the proposed methods will work for any objective function of the AC OPF problem as they do not depend on it. Lastly, while the QC relaxation (7) is given here as an example, the developed techniques can be used for any relaxation that utilizes bounds on variables.

A. Bound tightening based on line flow constraints

The bounds on the phase angle difference for a given branch can be obtained from the feasible set of its thermal limit constraint. Consider a branch between buses i and j represented by a π-model with admittance $g_{ij} + jb_{ij}$ and shunt susceptance b^s_{ij}. For simplicity, all formulations will be given for transmission lines but they can be easily extended to transformers. The line current is a function of the complex voltages at both ends of the line. The current magnitude at the beginning of the line, denoted by I_{ij}, is given by:

$$I_{ij}(V_i, V_i, \theta_{ij}) = \big(a_1 V_i^2 + a_2 V_j^2 + 2V_i V_j \left(a_3 \sin\theta_{ij} - a_4 \cos\theta_{ij}\right)\big)^{1/2}, \tag{8}$$

where $a_1 := g_{ij}^2 + \left(b_{ij} + b^s_{ij}\right)^2$, $a_2 := g_{ij}^2 + b_{ij}^2$, $a_3 := b^s_{ij} g_{ij}$, and $a_4 := g_{ij}^2 + b_{ij}^2 + b^s_{ij} b_{ij}$. To ensure secure operation of the grid, the value of I_{ij} is constrained to be below a given limit:

$$I_{ij}(V_i, V_j, \theta_{ij}) \le I_{ij}^{\max}. \tag{9}$$

This inequality corresponds to constraint (2h) in the AC OPF problem formulation. Let $\mathcal{I}$ denote the feasible set of (9). The boundary of $\mathcal{I}$ represents a surface that consists of all points for which (9) is binding. Therefore, it is implicitly defined as

$$I_{ij}(V_i, V_j, \theta_{ij}) = I_{ij}^{\max}. \tag{10}$$

Figure 1 shows an example of this boundary surface. Let $\bar{\theta}_{ij}$ denote the value of the phase angle difference for a point at the boundary. The expression for $\bar{\theta}_{ij}$ as a function of V_i and V_j was derived in [22] and is given by

$$\bar{\theta}_{ij}(V_i, V_j) = \arcsin\left(\frac{-a_3 t \pm |a_4|\sqrt{4a_1a_2 - t^2}}{2a_1a_2}\right), \tag{11}$$

where $t := a_1 V_i/V_j + a_2 V_j/V_i - (I_{ij}^{\max})^2/(V_i V_j)$. The algorithm for computing the bounds on θ_{ij} is based on the analysis of the properties of (9) and (11).

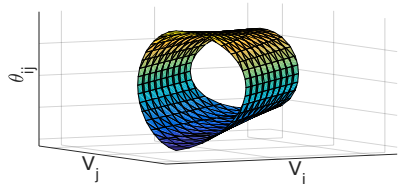

Fig. 1. Boundary of feasible set of line flow constraint

It was shown in [22] that for any pair of (V_i, V_j) for which $4a_1a_2 - t^2 > 0$, equation (11) has two distinct real-valued solutions denoted by $\bar{\theta}^-_{ij}$ and $\bar{\theta}^+_{ij}$. For such pairs of (V_i, V_j), constraint (9) is satisfied for $\forall\theta_{ij} \in \left[\bar{\theta}^-_{ij}, \bar{\theta}^+_{ij}\right]$. Hence, $\mathcal{I}$ lies inside the surface depicted in Figure 1. Let $\mathcal{V}$ denote the set of pairs (V_i, V_j) that satisfy voltage magnitude constraints (2f). Then, the values of θ_{ij} that belong to $\mathcal{I} \cap (\mathcal{V} \times \mathbb{R})$ are bounded by the following lower θ^l_{ij} and upper θ^u_{ij} limits:

$$\begin{aligned} \theta^l_{ij} &= \min\left\{\bar{\theta}^-_{ij}(V_i, V_j) \mid (V_i, V_j) \in \mathcal{V}\right\}, \\ \theta^u_{ij} &= \max\left\{\bar{\theta}^+_{ij}(V_i, V_j) \mid (V_i, V_j) \in \mathcal{V}\right\}. \end{aligned} \tag{12}$$

In order to compute (12) efficiently, let us further investigate the properties of the boundary of $\mathcal{I}$. Consider a new coordinate system proposed in [22] wherein the axes in the (V_i, V_j) plane are rotated counterclockwise by $\varphi = \arctan\sqrt{a_1/a_2}$, where $0 < \varphi < \pi/2$. Let x_1 and x_2 denote the new axes (see Figure 2a). In the new coordinate system, (9) can be expressed as

$$I_{ij}(x_1, x_2, \theta_{ij}) \le I_{ij}^{\max}. \tag{13}$$

Figure 2b shows the boundary surface of the feasible set of (13), which is simply a rotated boundary surface of (9). An example of the cross-section of this surface along the x_1 axis is visualized in Figure 2c. It suggests that the value of $\bar{\theta}^-_{ij}$ monotonically increases, whereas the value of $\bar{\theta}^+_{ij}$

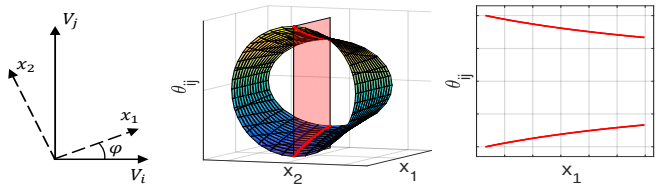

(a) Rotation of axes (b) Boundary surface (c) Cross-section

Fig. 2. Boundary in rotated coordinates and its cross-section along x_1 axis

monotonically decreases. It can be straightforwardly proven that this property holds for any intersection of the boundary surface along the x_1 and for any branch parameters, i.e.

$$\frac{\partial \bar{\theta}_{ij}^{+}(x_1,x_2)}{\partial x_1} \leq 0, \quad \frac{\partial \bar{\theta}_{ij}^{-}(x_1,x_2)}{\partial x_1} \geq 0, \quad \forall (x_1,x_2) \in \mathcal{I}_x, \tag{14}$$

where $\mathcal{I}_x$ is the projection of $\mathcal{I}$ onto the (x_1, x_2) plane. This means that θ_{ij} in set $\mathcal{I} \cap (\mathcal{V} \times \mathbb{R})$ reaches its minimum and maximum values at point (x_1, x_2) that belongs to $\mathcal{V}$ and has the minimum value of x_1. Since the axes x_1 and x_2 represent the rotation of the axes V_i and V_j with angle $0 < \varphi < \pi/2$, the extrema of θ_{ij} in $\mathcal{I} \cap (\mathcal{V} \times \mathbb{R})$ occur at $V_i = V_i^{\min}$ and/or $V_j = V_j^{\min}$. Hence, θ_{ij}^{l} can be obtained by first solving

$$\begin{aligned} \underset{V_i}{\text{minimize}} \quad & \bar{\theta}_{ij}^{-}(V_i, V_j^{\min}) \\ \text{subject to} \quad & V_i^{\min} \leq V_i \leq V_i^{\max}, \end{aligned} \tag{15}$$

then solving

$$\begin{aligned} \underset{V_j}{\text{minimize}} \quad & \bar{\theta}_{ij}^{-}(V_i^{\min}, V_j) \\ \text{subject to} \quad & V_j^{\min} \leq V_j \leq V_j^{\max}, \end{aligned} \tag{16}$$

and taking θ_{ij}^{l} to be the minimum of (15) and (16). Obtaining θ_{ij}^{u} is similar. Globally optimal solutions of (15) and (16) can be obtained analytically from (11). The same procedure is repeated for the current constraint at the end of the line to obtain the maximum range of θ_{ij} from both (2h) and (2i).

The computational complexity of this method is linear with respect to the number of branches in the system because tightening each bound takes constant time. Naturally, the bounds for all θ_{ij} can be computed in parallel, which can further reduce the computation time. It is worth noting that the analysis of $\mathcal{I}$ can also help obtain the bounds on $V_i - V_j$.

B. Bound tightening based on envelopes of power flows

In this method, each bound is tightened by solving an optimization problem based on the convex relaxation of (2). Therefore, the core principle is similar to what is presented in [19] but the optimization problems are formulated in a different way to improve computational efficiency. As discussed in Section III, one can convexify the AC OPF problem by replacing the nonlinear terms in the power flow equations with their convex envelopes based on (3)-(6). Consider a different version of (3)-(6), whereby each envelope is linear and represents a parallelogram (for one-variable terms) or parallelepiped (for two-variable terms). The examples of proposed envelopes are shown in Figure 3 as shaded areas. Such a formulation allows representing the envelope of a function $f_i(x)$ as

$$\left\langle \widehat{f_i(x)} \right\rangle := \begin{cases} \check{x} \geq \alpha_i x + \beta_i^l, \\ \check{x} \leq \alpha_i x + \beta_i^u. \end{cases} \tag{17}$$

where i is the index of the nonlinear term in the list of all terms that enter the power flow equations, and the values of

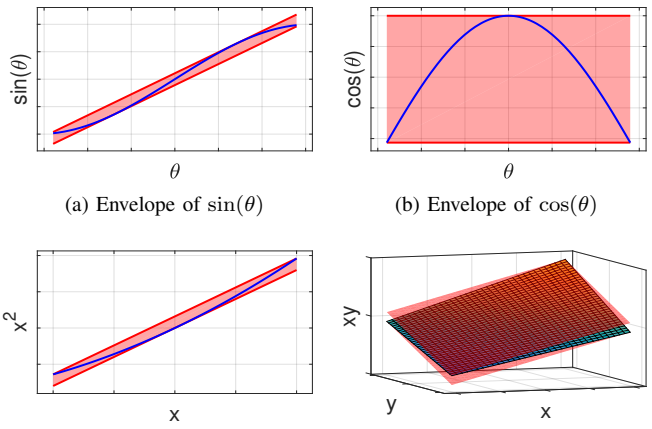

(a) Envelope of $\sin(\theta)$ (b) Envelope of $\cos(\theta)$

(c) Envelope of x^2 (d) Envelope of xy

Fig. 3. Proposed convex envelopes of trigonometric functions and monomials

TABLE I
PARAMETERS OF PROPOSED CONVEX ENVELOPES

	α	β^l	β^u
$\left\langle \widehat{\sin(x)} \right\rangle$	$\cos(\boldsymbol{x^m})$	$\boldsymbol{x^m}\cos(\boldsymbol{x^m}) - \sin(\boldsymbol{x^m})$	$-\boldsymbol{x^m}\cos(\boldsymbol{x^m}) + \sin(\boldsymbol{x^m})$
$\left\langle \widehat{\cos(x)} \right\rangle$	$\boldsymbol{\gamma_c}$	$-\boldsymbol{\gamma_c x^l} + \cos(\boldsymbol{x^l})$	$\boldsymbol{\gamma_c}\arcsin(\boldsymbol{\gamma_c}) + \sqrt{1-\boldsymbol{\gamma_c}^2}$
$\left\langle \widehat{x^2} \right\rangle$	$\boldsymbol{x^l} + \boldsymbol{x^u}$	$-(\boldsymbol{x^l} + \boldsymbol{x^u})^2/4$	$-\boldsymbol{x^l x^u}$
$\langle \widehat{xy} \rangle$	α_x: $(\boldsymbol{y^l} + \boldsymbol{y^u})/2$ α_y: $(\boldsymbol{x^l} + \boldsymbol{x^u})/2$	$-(\boldsymbol{x^l y^l} + \boldsymbol{x^u y^u})/2$	$-(\boldsymbol{x^l y^u} + \boldsymbol{x^u y^l})/2$

α_i, β_i^l and β_i^u for different envelope types are given in Table I. The envelope defined in (17) can also be represented as

$$\left\langle \widehat{f_i(x)} \right\rangle := \alpha_i x + \beta_i, \quad \beta_i^l \leq \beta_i \leq \beta_i^u, \tag{18}$$

Using (18), one can rewrite the power flow equations as

$$A \begin{bmatrix} \theta \\ V \end{bmatrix} = G \begin{bmatrix} P_G \\ Q_G \end{bmatrix} - \begin{bmatrix} P_D \\ Q_D \end{bmatrix} + C\beta, \tag{19}$$

where G is a generator-to-bus incidence matrix, matrices A and C are based on the system admittance matrix and the parameters of the convex envelopes defined in Table I. Matrix A is square but singular due to the rotational invariance of (19) with respect to θ. Let $\theta_i := 0$ and let us replace the i-th active power balance equation with constraint $\theta_i = 0$. This can only increase the set of feasible values of V and θ, and results in the following system:

$$\widetilde{A} \begin{bmatrix} \theta \\ V \end{bmatrix} = \widetilde{G} \begin{bmatrix} P_G \\ Q_G \end{bmatrix} - \begin{bmatrix} \widetilde{P}_D \\ Q_D \end{bmatrix} + \widetilde{C}\beta, \tag{20}$$

where $\widetilde{A}$ is A with its i-th row and column replaced with vectors whose i-th entry is one and rest are zero, and the tilde sign over other vectors/matrices means that their i-th element/row was replaced with zero(s). Since $\widetilde{A}$ is square and invertible, θ_{ij} can be obtained as

$$\theta_{ij} = \left(\left(\widetilde{A}^{-1}\right)_i - \left(\widetilde{A}^{-1}\right)_j \right) \left(\widetilde{G} \begin{bmatrix} P_G \\ Q_G \end{bmatrix} - \begin{bmatrix} \widetilde{P}_D \\ Q_D \end{bmatrix} + \widetilde{C}\beta \right), \tag{21}$$

where $(\widetilde{A}^{-1})_i$ and $(\widetilde{A}^{-1})_j$ are the i-th and j-th rows of the inverse of matrix $\widetilde{A}$. Let $z := [P_G, Q_G, \beta]$ denote the vector of variables, whose lower and upper bounds z^l and z^u are known from (2d)-(2e) and (18). Then, (21) can be rewritten as

$$\theta_{ij} = d^T z + d_0, \tag{22}$$

where d is a known vector and d_0 is a known scalar. The

lower(upper) bound on θ_{ij} can be obtained by solving

$$\begin{aligned} &\text{minimize(maximize)} \;\; d^T z + d_0 \\ &\underset{z}{\text{subject to}} \qquad\qquad z^l \leq z \leq z^u. \end{aligned} \tag{23}$$

The advantage of the formulation of (23) is that it can be solved by inspection, i.e. the objective is maximized if $z_i = z_i^l$ for any $d_i < 0$ and $z_i = z_i^u$ for any $d_i \geq 0$. Therefore, the solution algorithm for (23) has low computational complexity.

The proposed bound tightening method can be summarized as follows. First, the convex envelopes are computed using the initial variable bounds, and matrix $\widetilde{A}^T$ is factorized into $\widetilde{A}^T = LU$. Then, for each θ_{ij} the value of $(\widetilde{A}^{-1})_i - (\widetilde{A}^{-1})_j$ is obtained by solving $LUp_{ij} = e_{ij}$, where the i-th element of e_{ij} is 1, the j-th element is -1, and the rest are zero. Next, d and d_0 are computed and problem (23) is solved by inspection. Finally, the bounds are updated for those branches, for which the solution of (23) yields tighter bounds. Based on the new bounds, the convex envelopes are recomputed and the process is repeated iteratively until no further tightening is possible.

Since at each iteration matrix $\widetilde{A}$ is factorized only once, tightening each bound requires only several matrix-vector multiplications, with all matrices being sparse. In addition, each bound can be tightened in parallel, further improving the computational efficiency of the proposed algorithm. It is worth noting that this method can also be used for tightening the bounds on voltage magnitudes and their differences.

C. Bound tightening based on envelopes of bus currents

This method also tightens the bounds through optimization problems based on the relaxation of the power flow equations. The difference from the previous method is in how these problems are formulated. Consider the system of the power flow equations represented in the following form:

$$Y\underline{V} = \underline{I}, \tag{24}$$

where $Y := G + jB$ is the admittance matrix, $\underline{V} := V' + jV''$ and $\underline{I} := I' + jI''$ are the vectors of complex bus voltages and injection currents. The prime and double prime superscripts denote the real and imaginary parts of a complex value, respectively. The idea behind tightening the bounds on each θ_{ij} is to formulate a convex optimization problem that only includes constraints on I' and I'' and admits a fast solution.

First, the process of obtaining the convex constraints on I' and I'' is explained. Consider bus $i \in \mathcal{N}$, whose active and reactive power injections are denoted by P_i and Q_i, respectively. Then the value of $\underline{I}_i$ is given by

$$\underline{I}_i = \frac{P_i - jQ_i}{V_i' - jV_i''}. \tag{25}$$

One can construct a convex constraint on I_i' and I_i'' using the fact that P_i and Q_i are either constant (for a load) or bounded (for a generator), and $V_i^{\min} \leq V_i \leq V_i^{\max}$. The feasible set of this constraint should be as small as possible to obtain tighter bounds on phase angle differences from (24). To formulate a convex constraint with a small feasible set, let us install a shunt $y_i^{\text{sh}} := g_i^{\text{sh}} + jb_i^{\text{sh}}$ at bus i and replace $\underline{I}_i$ with an unknown current $\triangle\underline{I}_i := \triangle I_i' + j\triangle I_i''$ and a current flowing into y_i^{sh}:

$$\underline{I}_i = \triangle\underline{I}_i - y_i^{\text{sh}}\underline{V}_i. \tag{26}$$

Here, $\triangle\underline{I}_i$ is needed to compensate for variable P_i and Q_i and for the dependency of the shunt current on the magnitude of V_i. The goal is to select g_i^{sh} and b_i^{sh} such that they help impose the tightest possible constraint on $\triangle I_i'$ and $\triangle I_i''$ of the form

$$(\triangle I_i')^2 + (\triangle I_i'')^2 \leq \rho_i \tag{27}$$

while ensuring that (26) together with this constraint and the bounds on V_i is a relaxation of (25). Since $\triangle\underline{I}_i = \underline{I}_i + y_i^{\text{sh}}\underline{V}_i$, the optimal values of g_i^{sh}, b_i^{sh} can be obtained by solving the following optimization problem:

$$\underset{\substack{V_i', V_i'', P_i, \\ Q_i, g_i^{\text{sh}}, b_i^{\text{sh}}}}{\text{maximize}} \;\; \left(\Re\left(\underline{I}_i + y_i^{\text{sh}}\underline{V}_i\right)\right)^2 + \left(\Im\left(\underline{I}_i + y_i^{\text{sh}}\underline{V}_i\right)\right)^2 \tag{28a}$$

$$\text{subject to} \;\; V_i^{\min} \leq \sqrt{(V_i')^2 + (V_i'')^2} \leq V_i^{\max} \tag{28b}$$

$$P_i^l \leq P_i \leq P_i^u \tag{28c}$$

$$Q_i^l \leq Q_i \leq Q_i^u \tag{28d}$$

whose optimal objective value yields the value of ρ_i. Here, $\underline{I}_i$ is as defined in (25), $\Re(\cdot)$ and $\Im(\cdot)$ denote operators that return real and imaginary part of a complex value, respectively, and P_i^l, Q_i^l, P_i^u, Q_i^u are the lower and upper bounds on the active and reactive power injections at bus i. If bus i is a load bus, i.e. P_i and Q_i are constant, problem (28) can be solved analytically and the solution is given by

$$\begin{aligned} g_i^{\text{sh}} &:= -\frac{P_i}{V_i^{\min}V_i^{\max}}, \;\; b_i^{\text{sh}} := \frac{Q_i}{V_i^{\min}V_i^{\max}}, \\ \rho_i &:= \left(P_i^2 + Q_i^2\right)\left(\frac{V_i^{\max} - V_i^{\min}}{V_i^{\min}V_i^{\max}}\right)^2. \end{aligned} \tag{29}$$

Observe that the smaller the range of V_i is, the tighter (27) becomes, with $\triangle\underline{I}_i = 0$ for $V_i^{\min} = V_i^{\max}$. Hence, for typical operating limits on V_i the feasible set of (27) is small.

If bus i is a generator bus, an analytical solution of problem (28) is difficult to obtain. Since this problem is non-convex, an NLP solver may return its local optimum, which does not guarantee that (26), (27) and the bounds on V_i represent a relaxation of (25). To prevent this, problem (28) is simplified by assuming the following values of g_i^{sh} and b_i^{sh}:

$$g_i^{\text{sh}} := -\frac{P_i^l + P_i^u}{2V_i^{\min}V_i^{\max}}, \;\; b_i^{\text{sh}} := \frac{Q_i^l + Q_i^u}{2V_i^{\min}V_i^{\max}}, \tag{30}$$

which are related to the operation of a generator at the middle point of its feasible set of P_i and Q_i. While the resulting problem is still non-convex, it can be reformulated such that it has only three variables, namely, P_i, Q_i, and V_i. Since these variables are bounded and the objective function is smooth, the value of ρ_i can be obtained by a sampling method.

Applying this procedure to each bus, one can rewrite the system of power flow equations as

$$\hat{Y}\underline{V} = \triangle\underline{I}, \tag{31}$$

where $\hat{Y}_{ij} = Y_{ij}$ for all $i \neq j$ and $\hat{Y}_{ii} = Y_{ii} + y_i^{\text{sh}}$.

Now, the algorithm to tighten bounds on θ using (31) is explained. Consider branch $(i, j) \in \mathcal{L}$ and let bus j be the reference bus, i.e. $V_j'' = 0$ and $V_j = V_j'$. Assuming that $\hat{Y}$ is invertible, $\underline{V}_i$ is given by

$$\underline{V}_i = (\hat{Y}^{-1})_i \triangle\underline{I}, \tag{32}$$

where $(\hat{Y}^{-1})_i$ is the i-th row of the inverse of $\hat{Y}$. Let this row be denoted by $\underline{d} := d' + jd''$. It can be obtained from solving $\hat{Y}^T\underline{d} = e_i$, where e_i is a corresponding unit vector. Since by design vector $\underline{V}_j$ lies along the real axis, θ_{ij}^u can

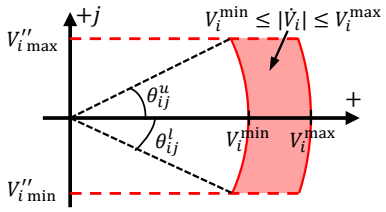

Fig. 4. Boundary of feasible set of line flow constraint

be obtained from maximizing the value of V_i'' (see Figure 4). The maximum value of V_i'', denoted by $V_{i\max}''$, is obtained as the optimal objective value of the following problem:

$$\begin{aligned} \underset{\triangle I', \triangle I''}{\text{maximize}} \quad & (d'')^T \triangle I' + (d')^T \triangle I'' \\ \text{subject to} \quad & (\triangle I_k')^2 + (\triangle I_k'')^2 \le \rho_k, \quad k \in \mathcal{N}. \end{aligned} \tag{33}$$

Problem (33) can be solved analytically and its optimal objective value is given by $V_{i\max}'' = \sum_k \rho_k \sqrt{(d_k')^2 + (d_k'')^2}$. Finally, as follows from Figure 4:

$$\theta_{ij}^u = \arcsin\left(\frac{V_{i\max}''}{V_i^{\min}}\right). \tag{34}$$

The value of θ_{ij}^l is obtained analogously.

Note that in reality matrix $\hat{Y}$ may be singular. To make it invertible, a special procedure is used whereby one column and one row are removed, whose indices depend on the branch. The details of this procedure are omitted due to space limitations. As with the other two methods, the bounds on θ_{ij} for all branches can be tightened in parallel.

V. Implementation

The proposed bound tightening algorithms were implemented as a MATLAB package, which was made open-source and is available on Github[1]. It requires that MATPOWER [23] be installed and the input test case be in the MATPOWER format. The interface function has a wide range of control options over the algorithms, which can help the user to choose a desired trade-off between the solution quality and computation time. In addition, the package can optionally use the KLU algorithm [24], which is part of SuiteSparse distribution and is specifically designed to efficiently solve linear systems related to circuits. This can help significantly accelerate certain computations. The interface function returns the MATPOWER structure with the tightened bounds on phase angle differences stored in the corresponding field.

VI. Numerical Experiments

A. Experimental setup

Numerical experiments were carried out using test cases of various sizes available in MATPOWER v6.0 and NESTA v0.5.0 [25]. Unless the bounds on branch phase angle differences were specified in the test case, their initial values were set to the steady-state limit of $\pm\pi/2$. The experimental results were obtained on a 2.8GHz four-core PC with 32GB of RAM. The QC relaxation of the AC OPF problem was solved by Gurobi through its MATLAB interface. To check the quality of the relaxation solution, the power flow (PF) problem was solved in MATPOWER using simultaneous PV/PQ switching

[1]https://github.com/dmitry-shchetinin/BTOPF

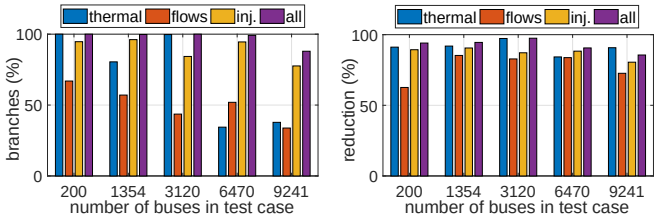

(a) Percentage of tightened bounds (b) Average reduction in range

Fig. 5. Comparison of effectiveness of proposed bound tightening methods

TABLE II
Computation times for proposed bound tightening methods

Case	Total time, s	Relative time of each method, %		
		thermal	power flows	bus currents
illinois200	0.29	16.4	57.7	30.0
1951rte	3.30	10.2	58.4	31.5
3120sp	9.19	6.93	50.9	42.2
6470rte	44.2	1.34	66.5	32.1
9241pegase	151.4	0.77	71.4	27.8

of all generator nodes with reactive power violations. The AC OPF problem was solved by IPOPT with the linear solver MA57 through its MATPOWER interface.

B. Analysis of proposed bound tightening methods

First, the performance of the proposed bound tightening methods was analyzed using five grids of various sizes, from 200 buses to over 9000 buses (see Table II for case names). For each grid, four experiments were carried out. In the first three, all bounds were tightened using only one of the proposed methods, while in the last experiment the combination of all three methods was used. Figure 5 presents the results of these experiments. The percentage of branches for which lower and/or upper bounds were tightened is shown in Figure 5a. Naturally, the combination of all three methods produced the best results with almost 100% tightened bounds for all but the largest test case. It was followed by the method based on envelopes of bus currents. Note that the results of the method based on thermal limits have the largest variance because this method requires the value of the thermal limit to be known. While in reality this is the case for all branches, for some of the test grids only a fraction of branches have thermal limits. Figure 5b presents the average relative reduction in the distance between the bounds, i.e. the average reduction in the feasible range of θ_{ij}. Note that it is only computed for those branches for which at least one of the bounds was tightened, which is why the method based on thermal limits achieved better average reduction than all methods combined. One can see that all methods were able to significantly tighten the bounds, reducing the range on average by 80-90%.

The computation times for the combination of all three methods are shown in Table II, which also details the relative time of each method. These results were obtained using parallel computations with four workers. One can see that the method based on the thermal limits was the fastest, followed by the method based on the envelopes of bus currents. The method based on the envelopes of power flows was the slowest due to the larger size of the optimization problems that it solves. Observe that the relative time for the method based on the thermal limits progressively reduced as the system size increased. This occurred because its complexity is linear with

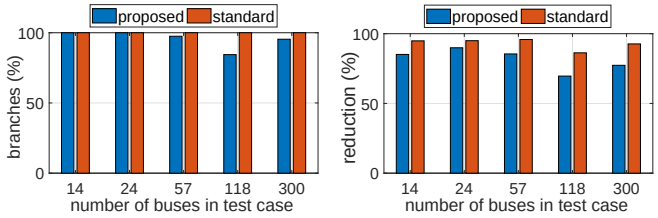

(a) Percentage of tightened bounds (b) Average reduction in range

Fig. 6. Comparison of proposed and standard bound tightening methods

TABLE III
COMPUTATION TIMES FOR PROPOSED AND STANDARD METHODS

Case	14	24	57	118	300
Time standard BT, s	7.53	42.8	175	868	5852
Time proposed BT, s	0.004	0.020	0.024	0.057	0.202
Speedup (x1000)	1.87	2.14	7.39	15.3	29.0

respect to the system size, whereas the complexity of the other two methods is super-linear. Overall, the computation times demonstrate that the proposed methods can be applied even to large-scale grids. Their efficiency could be further improved by increasing the number of parallel workers and implementing the algorithms in a lower level programming language.

The proposed bound tightening methods were then compared to the method presented in [19] (referred to as "standard") using five small-sized grids. For these experiments, the combination of all three proposed methods was used to tighten the bounds. Figure 6 presents the comparison of the percentage of tightened bounds and the average reduction in the feasible range of θ_{ij}. One can see that the standard method tightened more bounds and resulted in a higher range reduction compared to the proposed methods. This was expected because the standard method utilizes significantly more information by solving problem (7) with an objective of minimizing (maximizing) particular θ_{ij}. However, the difference in the percentage of tightened bounds was small in all but one case, and the proposed methods were able to capture 80-90% of the range reduction obtained by the standard method.

The advantage of the proposed methods lies in their computational efficiency. Table III presents the computation times for the standard and the combination of proposed methods as well as the speedup. These results were obtained using sequential tightening of all bounds. Clearly, the computation times could be significantly reduced through parallel computations. However, the speedup would stay roughly the same because the proposed methods can benefit from the parallelism in the same way that the standard method does. As the grid size increased, the proposed methods became progressively faster than the standard method, with the speedup reaching 29,000 times for the 300-bus system. Therefore, the proposed methods can be an attractive alternative to the standard method, in particular for large-scale grids. Note that the standard method was not tested on larger grids because of the high computation times.

C. Impact of bound tightening on quality of convex relaxation

Next, the impact of bound tightening (BT) on the quality of QC relaxation was analyzed using fifteen large-scale test cases: five from MATPOWER and ten from NESTA. Half of these NESTA cases represent congested operating conditions ("api") and the other half represent operating conditions with small branch angle differences ("sad"). Smaller test cases were not considered because they were examined in other studies, e.g. [18]. For each considered test case, the QC relaxation of the AC OPF problem was solved, first without BT and then with the proposed BT methods as a preprocessing step. The obtained results are presented in Table IV. The reported runtime of the QC relaxation with BT includes the BT time. One can see that BT increased the runtime of the QC OPF in most of the cases. However, the BT added only 3-9 seconds, the rest being due to a longer time spent solving the QC relaxation with Gurobi.

To assess the quality of the QC solution, its objective function value was compared to the value obtained by solving the original non-convex AC OPF problem with IPOPT. One can see that BT reduced their difference, referred to as optimality gap, in all test cases. However, the optimality gap alone cannot serve as an indicator of the relaxation quality because IPOPT can return a locally optimum point, in which case there would be a nonzero gap even if the relaxation was tight. Therefore, another metric was used to measure the quality of the relaxation solution. The values of complex voltages and generator outputs returned by the QC OPF were plugged into the power balance equations and the absolute values of the resulting bus mismatches were measured. Table IV reports the maximum and average values of these active and reactive power mismatches. As can be seen, BT helped significantly reduce the maximum and average active power mismatches for all test cases. The values of the average active power mismatches for the QC solution with BT indicate that the active power balances were close to being satisfied for many buses in several test cases. On the other hand, BT led to an increase in the reactive power mismatches for almost half of the cases. This occurred because in transmission grids reactive power is mostly influenced by voltage magnitudes, the bounds on which were not tightened. Nevertheless, BT had an overall positive effect on the apparent power mismatches.

Lastly, the usefulness of the solution of QC relaxation with and without BT was assessed. To do this, the PF problem was solved with the active power dispatch and generator voltage set-points taken from the relaxation. The starting values for the voltage magnitudes and angles were set to the corresponding values obtained by the relaxation. The number of iterations until convergence was measured and if the algorithm converged, the number of violations of voltage magnitude constraints (2f) was computed. The results are presented in the last four columns of Table IV. One can see that BT helped the PF solver recover a physically meaningful operating point, with fewer iterations and only one unsolved case compared to five such cases when BT was not used. In addition, BT helped reduce the number of violations of voltage constraints in all but one case. While the details of these violations are omitted due to space limitations, BT also helped make them less severe. The same applied to the thermal limit constraints. Note that the PF solver typically failed when using the flat start, regardless of whether BT was used before solving the relaxation.

VII. CONCLUSION

This paper presents three complementary, highly parallelizable, computationally efficient methods for tightening bounds on branch angle differences. The idea behind all methods is to tighten each bound through solving a convex optimization

TABLE IV
ANALYSIS OF IMPACT OF BOUND TIGHTENING ON QUALITY OF SOLUTION OF QC RELAXATION OF AC OPF PROBLEM

Case	QC OPF runtime, seconds		Optimality gap w.r.t. AC OPF solution, %		Bus power mismatch of QC OPF solution, p.u. (S_{base}=100MVA)								PF problem with QC OPF solution as starting point			
					active				reactive				iterations		V violations	
					maximum		average		maximum		average					
	no BT	w. BT	no BT	w. BT	no BT	w. BT	no BT	w. BT	no BT	w. BT	no BT	w. BT	no BT	w. BT	no BT	w. BT
1354pegase	22.4	47.3	0.075	0.061	21.8	16.1	1.06	0.36	3.75	11.2	0.23	0.32	16	12	41	33
1951rte	54.7	101.7	0.070	0.039	93.2	7.24	1.29	0.19	36.9	11.4	0.30	0.20	18	8	579	78
2383wp	68.6	108.6	0.693	0.517	347	2.14	5.57	0.05	5.71	10.9	0.13	0.34	—	12	—	54
2868rte	66.8	85.3	0.064	0.039	58.4	6.23	0.87	0.17	32.1	11.7	0.23	0.23	26	14	784	198
3120sp	85.0	96.3	0.502	0.312	318	3.34	2.20	0.10	55.5	14.5	0.28	0.22	20	12	20	3
1460wp_eir__api	37.4	44.9	1.263	1.257	1669	371	5.54	0.64	62.3	371	0.70	2.12	—	—	—	—
2224_edin__api	37.8	95.9	1.593	1.177	1965	4.95	5.29	0.16	30.4	25.4	0.24	0.24	—	6	—	59
2383wp_mp__api	56.7	105.8	0.744	0.391	383	3.58	7.73	0.06	11.4	16.5	0.21	0.31	—	9	—	0
2746wop_mp__api	41.0	48.2	0.249	0.186	383	2.75	5.16	0.08	41.3	9.83	0.55	0.18	10	9	0	0
3120sp_mp__api	74.0	132.2	1.315	0.896	321	1.54	5.34	0.08	56.5	5.96	0.65	0.19	10	9	2	0
1460wp_eir__sad	48.9	50.8	2.670	1.410	311	26.2	2.98	0.14	311	2694	2.05	5.72	21	15	250	170
2224_edin__sad	95.1	128.8	4.834	3.178	1115	4.55	4.44	0.12	26.2	31.0	0.22	0.26	24	16	103	114
2383wp_mp__sad	76.8	91.8	2.626	2.316	213	2.06	8.75	0.07	11.2	15.2	0.29	0.35	27	15	19	17
2746wop_mp__sad	117.4	131.0	2.533	2.088	226	4.31	5.96	0.13	72.8	42.1	0.72	0.24	—	23	—	133
3120sp_mp__sad	97.3	78.7	2.446	2.110	182	1.53	4.95	0.06	32.8	9.19	0.62	0.18	15	9	6	2

— - PF solver did not converge

problem that admits a fast solution. The first method tightens a given bound by using only the parameters of the corresponding branch, whereas the other two utilize the information of the entire system. These methods are made publicly available as an open-source MATLAB-based package.

The numerical experiments demonstrated that the proposed methods helped significantly tighten the bounds for the majority of branches in the system. The distance between lower and upper bounds was reduced on average by 80-90%, which is only slightly worse than the result produced by the standard optimization-based bound tightening. The computation time for the proposed methods was relatively low even for large-scale grids, particularly compared to the time required to solve the QC relaxation of the AC OPF problem. In addition, the experimental results showed that tighter bounds improved the quality of the QC relaxation by reducing the optimality gap and making its solution more useful.

Possible future work includes further improvement of the proposed techniques and their extension to the security-constrained OPF problem.

REFERENCES

[1] J. Carpentier, "Contribution á l'étude du dispatching économique", *Bulletin de la Société Française des Électriciens*, vol. 3, no. 8, pp. 431–447, 1962.

[2] F. Capitanescu et al, "State-of-the-art, challenges, and future trends in security constrained optimal power flow", *Electric Power Systems Research*, vol. 81, no. 8, pp. 1731–1741, 2011.

[3] Florin Capitanescu, "Critical review of recent advances and further developments needed in AC optimal power flow", *Electric Power Systems Research*, vol. 136, pp. 57–68, July 2016.

[4] Florin Capitanescu and Louis Wehenkel, "Experiments with the interior-point method for solving large scale Optimal Power Flow problems", *Electric Power Systems Research*, vol. 95, pp. 276–283, Feb. 2013.

[5] Anya Castillo and R. O'Neill, "Computational Performance of Solution Techniques Applied to the ACOPF", Tech. Rep., 2013.

[6] B. Stott and O. Alsac, "Optimal power flow: Basic requirements for real-life problems and their solutions", 2012.

[7] B. Stott, J. Jardim, and O. Alsac, "DC Power Flow Revisited", *IEEE Transactions on Power Systems*, vol. 24, no. 3, pp. 1290–1300, 2009.

[8] J. A. Momoh and J. Z. Zhu, "Improved interior point method for OPF problems", *IEEE Transactions on Power Systems*, vol. 14, no. 3, pp. 1114–1120, Aug. 1999.

[9] A. L. Motto, F. D. Galiana, A. J. Conejo, and J. M. Arroyo, "Network-constrained multiperiod auction for a pool-based electricity market", *IEEE Transactions on Power Systems*, vol. 17, no. 3, pp. 646–653, 2002.

[10] T.J. Overbye, Xu Cheng, and Yan Sun, "A comparison of the AC and DC power flow models for LMP calculations", in *Proceedings of the 37th Annual Hawaii International Conference on System Sciences*, 2004.

[11] K. Purchala, L. Meeus, D. Van Dommelen, and R. Belmans, "Usefulness of DC power flow for active power flow analysis", in *IEEE Power Engineering Society General Meeting, 2005*, 2005, pp. 454–459.

[12] R. Madani, S. Sojoudi, and J. Lavaei, "Convex Relaxation for Optimal Power Flow Problem: Mesh Networks", *IEEE Transactions on Power Systems*, vol. 30, no. 1, pp. 199–211, Jan. 2015.

[13] Masoud Farivar and Steven H. Low, "Branch Flow Model: Relaxations and Convexification—Part I", *IEEE Transactions on Power Systems*, vol. 28, no. 3, pp. 2554–2564, Aug. 2013.

[14] Carleton Coffrin, Hassan L. Hijazi, and Pascal Van Hentenryck, "The QC Relaxation: A Theoretical and Computational Study on Optimal Power Flow", *IEEE Transactions on Power Systems*, vol. 31, no. 4, pp. 3008–3018, July 2016.

[15] Javad Lavaei and Steven H. Low, "Zero Duality Gap in Optimal Power Flow Problem", *IEEE Transactions on Power Systems*, vol. 27, no. 1, pp. 92–107, Feb. 2012.

[16] M. Nick, R. Cherkaoui, J. Y. LeBoudec, and M. Paolone, "An Exact Convex Formulation of the Optimal Power Flow in Radial Distribution Networks Including Transverse Components", *IEEE Transactions on Automatic Control*, vol. PP, no. 99, pp. 1–1, 2017.

[17] C. Chen, A. Atamtürk, and S. S. Oren, "Bound Tightening for the Alternating Current Optimal Power Flow Problem", *IEEE Transactions on Power Systems*, vol. 31, no. 5, pp. 3729–3736, Sept. 2016.

[18] Carleton Coffrin, Hassan L. Hijazi, and Pascal Van Hentenryck, "Strengthening Convex Relaxations with Bound Tightening for Power Network Optimization", in *Principles and Practice of Constraint Programming*. Aug. 2015, Lecture Notes in Computer Science, pp. 39–57, Springer, Cham.

[19] C. Coffrin, H. L. Hijazi, and P. Van Hentenryck, "Strengthening the SDP Relaxation of AC Power Flows With Convex Envelopes, Bound Tightening, and Valid Inequalities", *IEEE Transactions on Power Systems*, vol. 32, no. 5, pp. 3549–3558, Sept. 2017.

[20] B. Kocuk, S. S. Dey, and X. A. Sun, "Inexactness of SDP Relaxation and Valid Inequalities for Optimal Power Flow", *IEEE Transactions on Power Systems*, vol. 31, no. 1, pp. 642–651, Jan. 2016.

[21] Garth P. McCormick, "Computability of global solutions to factorable nonconvex programs: Part I — Convex underestimating problems", *Mathematical Programming*, vol. 10, no. 1, pp. 147–175, Dec. 1976.

[22] D. Shchetinin, T. Tinoco De Rubira, and G. Hug, "On the Construction of Linear Approximations of Line Flow Constraints for AC Optimal Power Flow", *under second round of review in IEEE Transactions on Power Systems*, 2018.

[23] R. D. Zimmerman, C. E. Murillo-Sanchez, and R. J. Thomas, "MATPOWER: Steady-State Operations, Planning, and Analysis Tools for Power Systems Research and Education", *IEEE Transactions on Power Systems*, vol. 26, no. 1, pp. 12–19, Feb. 2011.

[24] Timothy A. Davis and Ekanathan Palamadai Natarajan, "Algorithm 907: KLU, A Direct Sparse Solver for Circuit Simulation Problems", *ACM Trans. Math. Softw.*, vol. 37, no. 3, pp. 36:1–36:17, Sept. 2010.

[25] Carleton Coffrin, Dan Gordon, and Paul Scott, "NESTA, The NICTA Energy System Test Case Archive", *CoRR*, vol. abs/1411.0359, 2014.